




ORIGINAL RESEARCH ARTICLE

Thermoelectric Properties of *n*-type GaN and 2D Electron Gas in AlGa_N-GaN Heterostructure

C. BRYAN ^{1,3} P. FAUCHERAND,¹ M. CHARLES,² M. PLISSONNIER,² and G. SAVELLI¹

1.—CEA-Liten, 17 Avenue des Martyrs, 38000 Grenoble, France. 2.—Univ. Grenoble Alpes, CEA, LETI, 38000 Grenoble, France. 3.—e-mail: charlotte.bryan@cea.fr

In this paper, the thermoelectric properties of *n*-type GaN and a 2D electron gas (2DEG) created from an AlGa_N/GaN heterostructure are presented. Their thermoelectric properties are essential in order to optimise the thermoelectric devices they are used for, such as thermoelectric sensors, generators or coolers. In this study, Seebeck coefficients of $-162 \mu\text{V/K}$ and $-86 \mu\text{V/K}$ and power factor (σS^2) values of $0.56 \text{ mW}/(\text{m K}^2)$ and $3.1 \text{ mW}/(\text{m K}^2)$ were obtained for *n*-type GaN and the AlGa_N/GaN heterostructure, respectively, at 430 K. Their Seebeck coefficient and resistivity were also measured over a number of temperature cycles, with no change in either of these measurements during the cycling, implying that these materials are thermoelectrically stable. Seebeck coefficients and thermoelectric properties of both materials remain stable throughout the temperature changes. These characteristics show the suitability of these materials for high performance thermoelectric sensors.

Key words: Thermoelectric properties, III-N materials, 2DEG, thermoelectric sensors

INTRODUCTION

Thermoelectric materials convert heat into electricity and electricity into heat. Their figure of merit (ZT) is defined as¹:

$$ZT = \frac{S^2 \sigma T}{\kappa} \quad (1)$$

where S , σ , T and κ are the Seebeck coefficient, the electrical conductivity, absolute temperature, and thermal conductivity, respectively. A high ZT is required for efficient conversion from thermal to electrical energy, corresponding to a high Seebeck coefficient, high electrical conductivity and low thermal conductivity. Opposing trends between S , σ and κ typically exist: as σ increases, S decreases while increasing σ also increases κ . To achieve high thermoelectric performance, the power factor $\text{PF} = \sigma S^2$ is a key factor.

AlGa_N/GaN materials are of great interest for high power and high frequency application devices due to their electronic properties. These properties include a wide band gap, high saturation velocity and high breakdown field.² The large difference in polarisation between these two materials creates an accumulation of negative charges at the GaN surface next to the AlGa_N/GaN interface. This results in the formation of a two-dimensional electron gas (2DEG) which has low resistivity, high mobility and a high sheet carrier density. This 2DEG is commonly used for high electron mobility transistors (HEMTs).^{3,4} As for all transistors, if they are not well managed, overheating can occur, leading to the deterioration of their output signal, and even to thermal runaway, destroying the component.

An effective way to measure temperature changes and to manage the thermal exchange is by implementing in situ thermoelectric sensors. Thermoelectric sensors are composed of semi-conducting *p*-type and *n*-type lines connected electrically in series and thermally in parallel. Because of the Seebeck effect, a potential is generated which is proportional to the

(Received July 15, 2020; accepted November 25, 2020; published online January 4, 2021)

difference in temperature within the sensor's lines. This potential difference is calculated from:

$$U = N \times S_{np} \times \Delta T \quad (2)$$

or

$$U = N \times S_{np} \times \varphi \times R_{th} \quad (3)$$

where N , S_{np} , ΔT , φ and R_{th} are the number of junctions, the Seebeck coefficient of the two materials ($S_{np} = S_p - S_n$), the difference in temperature, the heat flow and the thermal resistance within the sensor, respectively. This type of integrated thermoelectric sensor has previously been developed using silicon based materials to measure CMOS transistor temperatures and heat flows.⁵ Thermoelectric sensors using III-N materials are now being developed in our laboratories for AlGaIn/GaN devices.

Thermoelectric sensors have several advantages compared to resistance temperature sensors, which are used in certain integrated circuits⁶:

1. No external energy is needed for thermoelectric sensors to generate a readable signal, in contrast to sensors that use I - V measurements to measure the resistance of a material, which increases with temperature.
2. Resistance sensors only measure a temperature at a specific time, while thermoelectric sensors can also measure a heat flow, which can be used to predict temperature variations (Eq. 3).
3. A more accurate measurement is obtained when sensors are placed closer to the transistor. In situ thermoelectric sensors are fabricated simultaneously with an HEMT so that the components can be placed very close together on an integrated circuit. Resistance sensors are not fabricated in situ so cannot be placed as close to the device as thermoelectric sensors.

In situ fabrication imposes many constraints, such as the choice of material: they must use the same materials as an HEMT, GaN or AlGaIn/GaN heterostructures in this case, and must follow the same fabrication and dimensioning rules. To design an efficient thermoelectric sensor, the thermoelectric properties of the material must be known. Only a few studies can be found on their thermoelectric behaviour as their application in the thermoelectric field has not yet been developed.⁷⁻¹¹ In this study, we measure the electrical properties and Seebeck coefficient of n -type GaN and an AlGaIn/GaN 2DEG.

METHOD

The structures were grown by metal-organic vapour phase epitaxy (MOVPE) on 200-mm-diameter silicon (111) substrates. An AlN nucleation layer is first grown on the substrate, followed by AlGaIn and GaN transition layers and an electrically

insulating carbon doped GaN layer. More details of the growth and crystal quality can be found.^{12,13} For the n -type GaN layer, a silicon doped GaN layer 1100 nm thick, with a doping level of $5 \times 10^{18} \text{ cm}^{-3}$ was grown on top of the carbon doped GaN, as shown Fig. 1a. For the AlGaIn/GaN heterostructure, a thicker carbon doped GaN layer was grown, followed by 100 nm GaN channel. The AlGaIn/GaN heterostructure was composed of a 0.7-nm-thick AlN layer and a 25-nm-thick $\text{Al}_{0.22}\text{Ga}_{0.78}\text{N}$, capped with an SiN_x passivation layer, as shown in Fig. 1b. The AlN "spacer" layer grown between the AlGaIn and GaN layers generates improved confinement of the electron gas and increased sheet carrier density. Its energy gap is 6.2 eV, creating a deeper and narrower well at the heterojunction compared with a structure without AlN spacer.

The Seebeck coefficient was obtained using a ZEM-3 ULVAC GmbH system. The measurement system functions as follows: the sample is held vertically in place between an upper and lower block. The sample is heated and held at a specified temperature. A gradient is then applied by heating only the lower block. The Seebeck coefficient is obtained by measuring the temperatures T_1 and T_2 with the two side thermocouples and then measuring the thermal electromotive force between the same two wires.

The electric resistance of the samples can also be measured using the ZEM-3 system with the four-terminal method. In this case, a current is applied at the ends of the sample and the voltage drop is determined between the side wires of the thermocouple.

Samples measuring 20 mm x 7 mm were used for these measurements, each with four contacts: two outer contacts for the current and two middle contacts for the thermocouples. The contacts used are described in a separate paper.¹⁴ For the n -type GaN material, contacts are deposited and then annealed at different temperatures. In the case of the AlGaIn/GaN heterostructure they are either deposited on the GaN layer after SiN , AlN and AlGaIn etching or deposited on the AlGaIn layer and annealed at 850°C to diffuse across the AlGaIn layer to the 2DEG.

To avoid any current going through the silicon substrate, electrically isolating tape is attached at both ends of the substrate and silver paint is used to electrically connect the upper and lower blocks to the outer contacts.

Electrical resistivity and charge mobility at ambient temperature were measured by a simultaneous Hall Effect and Van der Pauw method, which we call the VDPH measurement. VDPH measurements were performed on these samples to find the surface and volume concentration of carriers, electron mobility and electric resistivity. These measurements were performed at room temperature on 20 mm x 20 mm samples, with ohmic contacts as previously described located in each corner.

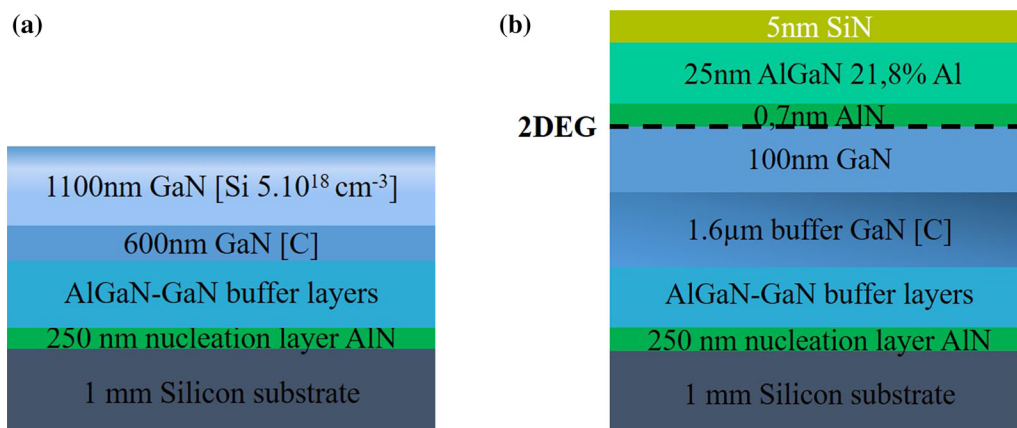


Fig. 1. Schematic representation of (a) the *n*-type GaN structure and (b) the AlGa_N/GaN structures.

RESULTS

Thermoelectric Property Measurements

The electrical properties, Seebeck coefficient and power factor for the two structures are presented in Tables I and II, and compared with data from literature.

Measurements were performed at temperatures from 350 K to 500 K corresponding to the typical operating temperature range of the transistor, with results of Seebeck coefficient and resistivity given for a temperature of 430 K (which can be considered the critical temperature for power circuits) in Tables I and II for *n*-type GaN and AlGa_N/GaN heterostructure, respectively.

The exact depth of the 2DEG is not known precisely; hence, density and resistance results for the 2DEG are given in surface concentration and sheet resistance. Its electrical resistance is also given in electrical resistivity assuming a 5-nm 2DEG depth for an easier comparison with the *n*-GaN material. The thickness of the 2DEG is calculated as being the region where the GaN is degenerated, i.e. the depth of the conduction band which is lower than the Fermi band.⁷ Values are comparable to those found in the literature, although not all growth parameters are the same—different Al concentrations in AlGa_N layer and different GaN and AlGa_N thickness lead to different electrical results. The Hall Effect measurements are also similar to previous measurements performed on similar structures.¹⁴

As expected, the 2DEG in the AlGa_N/GaN heterostructure has a lower electrical resistivity than the *n*GaN at both room temperature and at higher temperatures ($2.2 \times 10^{-4} \Omega \text{ cm}$ compared with $4.3 \times 10^{-3} \Omega \text{ cm}$ for the *n*-type GaN at room temperature).

Figure 2 shows the average values of the Seebeck coefficient for the *n*-type GaN and the AlGa_N/GaN heterostructure, with average values obtained from

measurements using the different contacts. We can see that the Seebeck coefficient is higher for *n*GaN than for the AlGa_N/GaN heterostructure across the whole temperature range.

As the voltage generated by a thermoelectric sensor is directly proportional to the Seebeck coefficient (Eqs. 2 and 3) and that the Seebeck coefficient of *n*GaN is higher than that of the AlGa_N/GaN heterostructure across the whole temperature range, the sensor's output will be more sensitive using *n*-GaN than using the AlGa_N/GaN heterostructure. Figure 3 shows the average electrical resistivity average and PF average, with average values obtained from measurements using the different contacts, as a function of the temperature. From Fig. 3, we see that the electrical resistivity of the AlGa_N/GaN heterostructure is much lower than that of the *n*GaN across the entire temperature range, and despite the lower Seebeck coefficient, the power factor is higher for the AlGa_N/GaN heterostructure. This will, therefore, also lead to a greater *PF*.

Temperature Cycles

The Seebeck coefficient and resistivity were measured using temperature cycles with temperatures ranging from 400 K to 520 K. Values were repeatedly taken over a number of temperature cycles. Figures 4 and 5 are examples of cyclic Seebeck coefficient, resistivity and *PF* measurements. The Seebeck coefficient, resistivity and consequently the power factor show reproducible results, which implies that the materials are thermoelectrically stable with temperature. There is a very slight variability between cycles, but no systematic shift across the cycles; therefore, this is due to errors within the measurement not due to changes in the materials. A thermoelectrically stable material is very important for temperature sensors in integrated circuits as they will be subject to many temperature cycles.

Table I. Electrical properties and Seebeck coefficient of *n*-type GaN

	Sheet concentration (cm^{-2}) 300 K	Bulk concentration (cm^{-3}) 300 K	Mobility ($\text{cm}^2/\text{V s}$) 300 K	Electrical resistivity VDPH ($\Omega \text{ cm}$) 300 K	Electrical resistivity ZEM-3 ($\Omega \text{ cm}$) 430 K	Seebeck coefficient ($\mu\text{V}/\text{K}$) 430 K	PF ($\text{mW m}^{-1} \text{K}^{-2}$) 430 K
n-GaN Literature ¹⁴	$5.4 \times 10^{14} \pm 0.4 \times 10^{14}$	$4.9 \times 10^{18} \pm 0.4 \times 10^{18}$ 2×10^{18}	220 ± 12 350	$4.3 \times 10^{-3} \pm 0.1 \times 10^{-3}$ 4×10^{-3}	$4.6 \times 10^{-3} \pm 2.5 \times 10^{-4}$ 1.42×10^{-2}	-162 ± 3 -105	0.56 ± 0.03 0.8^b

Table II. Electrical properties and Seebeck coefficient of the 2DEG created at the AlGaIn/GaN heterojunction

	Sheet concentra- tion (cm^{-2}) 300 K	Mobility ($\text{cm}^2/\text{V s}$) 300 K	Electrical sheet resistance (Ω/sq) 300 K	Electrical resistiv- ity VDPH ($\Omega \text{ cm}$) 300 K	Electrical resistivity ZEM-3 ($\Omega \text{ cm}$) 430 K	Seebeck coeffi- cient ($\mu\text{V}/\text{K}$) 430 K	PF ($\text{mW m}^{-1} \text{K}^{-2}$) 430 K
AlGaIn/GaN heterojunc- tion Literature ⁷	$7 \times 10^{12} \pm 0.6 \times 10^{12}$	2000 ± 100	438 ± 8	$2.2 \times 10^{-4} \pm 2 \times 10^{-5}$	$2.4 \times 10^{-4} \pm 1.3 \times 10^{-5}$	-86 ± 4	3.1 ± 0.2
	8.5×10^{12}	1500	423	$1.7 \cdot 10^{-4}$		-120	9

CONCLUSION

Electrical properties including electron mobility, charge density and resistivity as well as the Seebeck coefficient were measured on two materials: *n*-type GaN and an AlGaN/GaN heterostructure. The Seebeck coefficient is found to be higher for the *n*-type GaN than for the AlGaN/GaN heterostructure, so ideally *n*-GaN material would be preferred for thermoelectric temperature sensors. However, as both Seebeck coefficients are high enough to make precise temperature measurements, for real devices it may be preferable to integrate these sensors with AlGaN/GaN heterostructures following a standard HEMT fabrication process.

Good reproducibility and stability of the Seebeck coefficient, not previously presented in the literature for GaN based materials, is shown here for *n*GaN and AlGaN/GaN heterostructures when measured over many temperature cycles. This is a very important criterion for devices that will endure a large number of temperature changes.

These results show that *n*GaN and AlGaN/GaN heterostructures are suitable materials for thermoelectric sensors, with high sensitivity and good stability. Because of the ability of these sensors to be directly integrated using existing fabrication processes, and as they do not require external energy input, these are very attractive for integration into GaN based power electronic circuits.

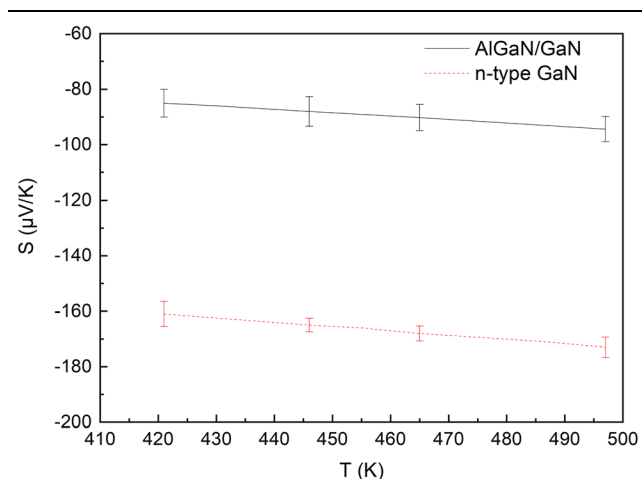


Fig. 2. Temperature dependence of the average Seebeck coefficient of *n*-type GaN and AlGaN/GaN heterostructure.

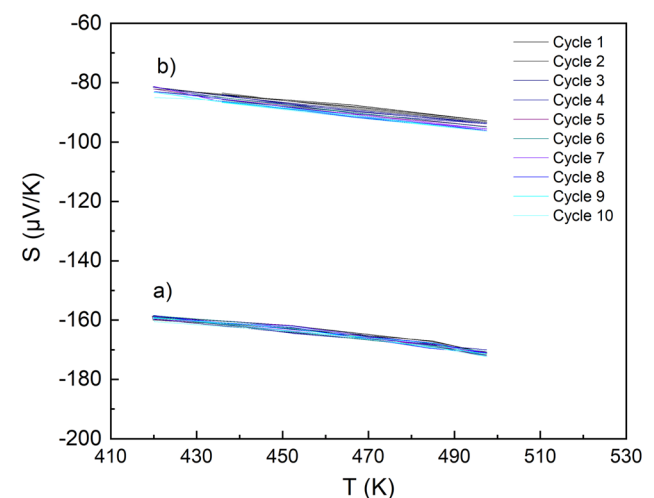


Fig. 4. Temperature dependence of the Seebeck coefficient over 10 cycles, for (a) *n*-type GaN with a Ti/Au/Al contact annealed at 735°C and (b) AlGaN/GaN heterostructure with a Ti/Al/Ni/Au contact annealed at 735°C.

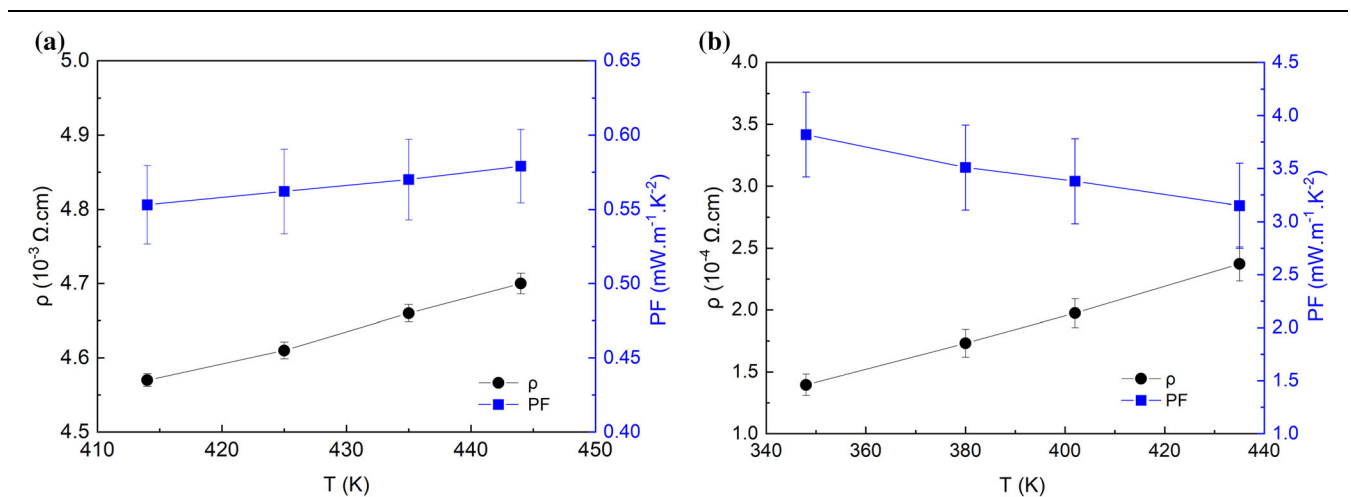


Fig. 3. Temperature dependence of the average resistivity and PF of (a) *n*-type GaN and (b) AlGaN/GaN heterostructure.

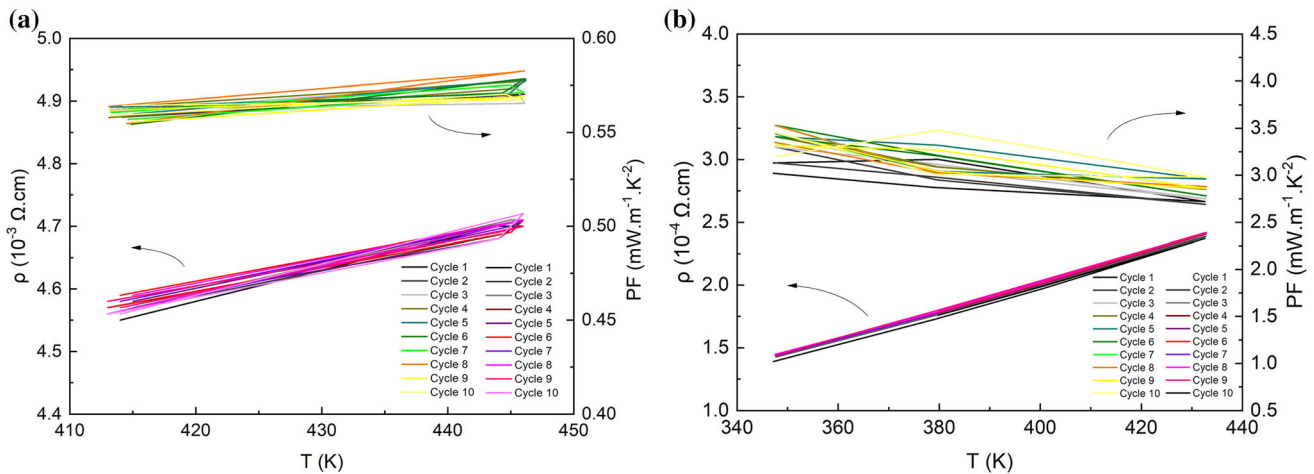


Fig. 5. Temperature dependence of the electrical resistivity and PF over 10 cycles for (a) n -type GaN with a Ti/Au/Al contact annealed at 735°C and (b) AlGaIn/GaN heterostructure with a Ti/Al/Ni/Au contact annealed at 735°C .

ACKNOWLEDGMENTS

The sample preparation has been performed with the help of the “Plateforme Technologique Amont”, Grenoble, France, with the financial support of the “Nanosciences aux limites de la Nanoélectronique” Foundation and CNRS Renatech network.

CONFLICT OF INTEREST

The authors declare that they have no conflict of interest.

REFERENCES

1. D.M. Rowe, *Thermoelectric Handbook* (Boca Raton: CRC, 2006).
2. B. Rowena, S.L. Selvaraj, and T. Egawa, *IEEE Electr Device L* 32, 11 (2011).
3. U.K. Mishra, S. Likun, T.E. Kazior, and Y.-F. Wu, *Proc. IEEE* 97, 2 (2007).
4. O. Ambacher, J. Smart, J.R. Shealy, N.G. Weimann, K. Chu, M. Murphy, W.J. Schaff, and L.F. Eastman, *J. Appl. Phys.* 85, 3222 (1999).
5. G. Savelli, J.-P. Colonna, M. Keller, P. Coudrain, D. Wendler, J. Goepfert, Y. Manoli, P. Faucherand, and A. Royer, *J. Phys. D: Appl. Phys.* 53, 445101 (2020).
6. C.C. Wang, Z.Y. Hou, and J.C. You, *Sensors* 18, 2165 (2018).
7. H. Ohta, S.W. Kim, S. Kaneki, A. Yamamoto, and T. Hashizume, *Adv. Sci.* 5, 1700696 (2018).
8. A. Szein, J.E. Bowers, S.P. DenBaars, and S. Nakamura, *Appl. Phys. Lett.* 104, 042106 (2014).
9. K. Nagase, S. Takado, and K. Nakahara, *Phys. Status Solidi A* 213, 4 (2016).
10. A.S. Yalamarthy, H. So, M.M. Rojo, A.J. Suria, X. Xu, E. Pop, and D.G. Senesky, *Adv. Funct. Mater.* 28, 22 (2018).
11. N. Maeda, K. Tsubaki, T. Saitoh, T. Tawara, and N. Kobayashi, *Opt. Mater.* 23, 1–2 (2003).
12. M. Charles, Y. Baines, S. Bos, R. Escoffier, G. Garnier, J. Kanyandekwe, J. Lebreton, and W. Vandendaele, *J. Cryst. Growth* 464, 164–167 (2017).
13. M. Charles, Y. Baines, A. Bavard, and R. Bouveyron, *J. Cryst. Growth* 89–93, 483 (2018).
14. I. Nifa, C. Leroux, A. Torres, M. Charles, D. Blachier, G. Reibold, G. Ghibaudo, and E. Bano, *Microelectron Eng.* 178, 128–131 (2017).

Publisher’s Note Springer Nature remains neutral with regard to jurisdictional claims in published maps and institutional affiliations.